

PAPER • OPEN ACCESS

Semi-automatic detection of the evolutionary forms of visceral leishmaniasis in microscopic blood smears

To cite this article: J Salazar *et al* 2019 *J. Phys.: Conf. Ser.* **1386** 012135

View the [article online](#) for updates and enhancements.



IOP | ebooks™

Bringing you innovative digital publishing with leading voices to create your essential collection of books in STEM research.

Start exploring the collection - download the first chapter of every title for free.

Semi-automatic detection of the evolutionary forms of visceral leishmaniasis in microscopic blood smears

J Salazar¹, M Vera¹, Y Huérfano², M I Vera², E Gelvez-Almeida¹, and O Valbuena^{1,3}

¹ Universidad Simón Bolívar, San José de Cúcuta, Colombia

² Universidad de Los Andes, San Cristóbal, Venezuela

³ Universidad de Pamplona, Pamplona, Colombia

E-mail: j.salazar@unisimonbolivar.edu.co

Abstract. Leishmaniasis is a complex group of diseases caused by obligate unicellular and intracellular eukaryotic protozoa of the leishmania genus. Leishmania species generate diverse syndromes ranging from skin ulcers of spontaneous resolution to fatal visceral disease. These syndromes belong to three categories: visceral leishmaniasis, cutaneous leishmaniasis and mucosal leishmaniasis. The visceral leishmaniasis is based on the reticuloendothelial system producing hepatomegaly, splenomegaly and lymphadenopathy. In the present article, a semi-automatic segmentation strategy is proposed to obtain the segmentations of the evolutionary shapes of visceral leishmaniasis called parasites, specifically of the type amastigote and promastigote. For this purpose, the optical microscopy images containing said evolutionary shapes, which are generated from a blood smear, are subjected to a process of transformation of the color intensity space into a space of intensity in gray levels that facilitate their subsequent preprocessing and adaptation. In the preprocessing stage, smoothing filters and edge detectors are used to enhance the optical microscopy images. In a complementary way, a segmentation technique that groups the pixels corresponding to each one of the parasites, presents in the considered images, is applied. The results reveal a high correspondence between the available manual segmentations and the semi-automatic segmentations which are useful for the characterization of the parasites. The obtained segmentations let us to calculate areas and perimeters associated with the parasites segmented. These results are very important in clinical context where both the area and perimeter calculated are vital for monitoring the development of visceral leishmaniasis.

1. Introduction

Leishmaniasis comprises a group of diseases caused by obligate unicellular and intracellular eukaryotic protozoa of the genus leishmania that mainly damage the reticuloendothelial system of the host. There are two evolutionary forms of leishmania: the flagellated extracellular promastigote in the sand-fly vector and the non-delayed intracellular amastigote in the vertebrate host, including humans. The promastigotes are injected by means of the proboscis of the female phlebotomize into the skin of the vertebrate host. Neutrophils are the first host cells to phagocytose promastigotes at the site of their inoculation [1].

Infected neutrophils undergo apoptosis by releasing viable parasites that are phagocytosed by macrophages or else the apoptotic cells themselves are phagocytosed by macrophages and dendritic cells. The parasites multiply as the amastigotes within the macrophages cause the cell to rupture,



subsequently invading other macrophages. The mosquito acquires amastigotes while feeding from the infected host and these become flagellated microorganisms within the posterior portion of the midgut and multiply by binary fission; then the promastigotes migrate to the anterior portion of the midgut and infect a new host when the mosquito is fed again. The syndromes, generated by leishmania, belong to three extensive categories: visceral leishmaniasis (VL), cutaneous leishmaniasis (CL) and mucosal leishmaniasis (ML) [1].

Due VL is the most severe form of leishmaniasis [2], this research focuses attention on the semiautomatic segmentation of the evolutionary shapes (parasites) associated with this type of leishmaniasis. The importance of this kind of research is the possibility of generate automatic strategies for detecting and monitoring efficiently the visceral leishmaniasis.

Additionally, Figure 1 shows the main medical imaging modalities used for diagnostic of several human pathologies.

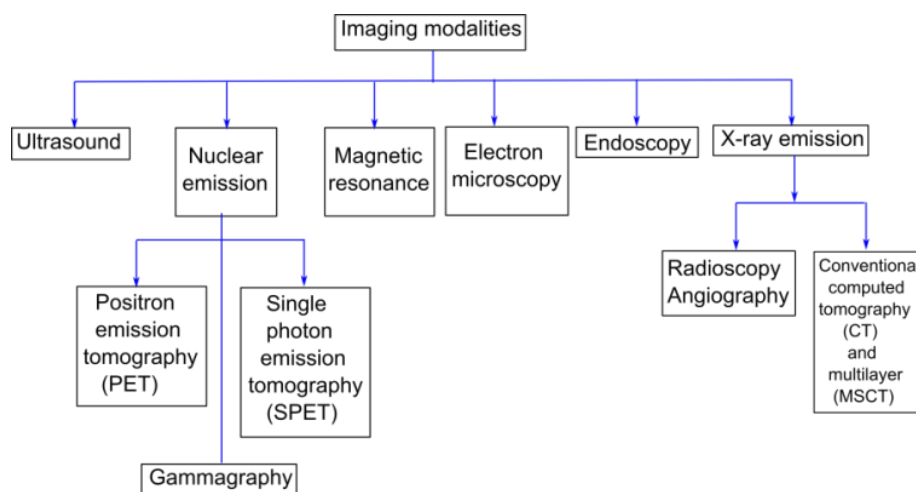


Figure 1. Imaging modalities used in the medical routine [3].

An example of these pathologies is the VL. In this paper, VL evolutionary forms are segmented considering bone marrow samples obtained from microscopic images.

Some researchers have addressed the issue of VL parasites segmentation. These papers have been biased towards the application of computational techniques using the following approaches: deformable models [2-5], thresholding [6] and deep learning [7].

In our paper, we use MSCT images and propose a semi-automatic computational strategy (SACS), based on the application of a filter bank and clustering technique for LV parasites segmentation.

2. Materials and methods

2.1. Dataset

A digital camera (Sony DSC-H9) coupled on an optical microscope (Olympus-CH40RF200) were used for VL data acquisition generating color images [8]. In this research, the data consists of nine original color images with three intensities channels identified as red (R), green (G) and blue (B) channels. These color images, usually, are called RGB images. Additionally, we have 9 annotated RGB images, which represent the ground truths used for SACS validation.

2.2. Computational strategy proposed

Figure 2 shows a block diagram of the semi-automatic computational strategy (SACS), proposed in this paper, for segmenting the typical leishmaniasis evolutionary shapes (LES).

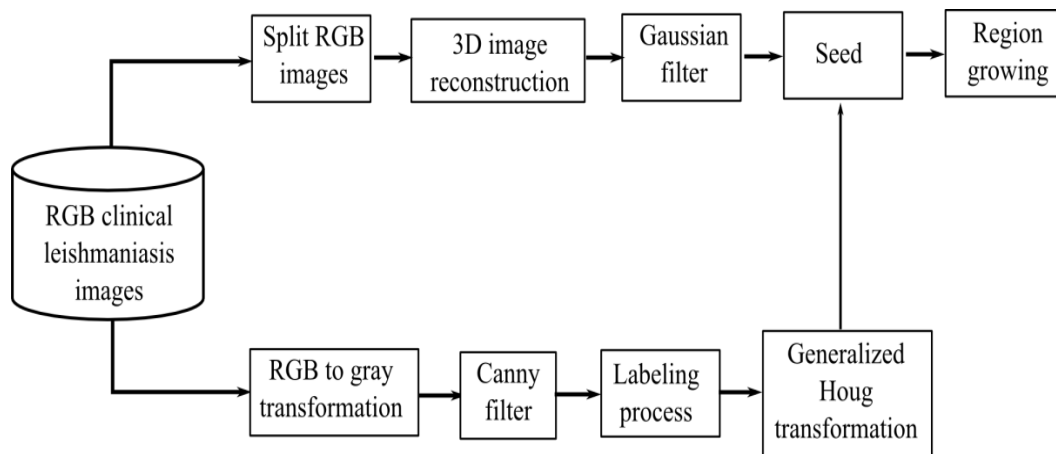


Figure 2. Block diagram of the proposed strategy (SACS).

2.2.1. Re-processing. At this stage, initially, a filter bank is applied to the dataset described in 2.1 section. A brief explanation of these filters is found below.

- Split RGB images. Due the inherent complexity of RGB images, in this paper, we decided to separate the red, green and blue channels of RGB images.
- 3D image reconstruction. Considering the channels images, we built a three dimensional (3D) datasets for using a 3D digital imaging processing.
- Gaussian filter. In this paper, the Gaussian filter smooths the 3D datasets by convolving it with a Gaussian kernel using as standard deviations, the standard deviation of original images [9]. A discrete Gaussian distribution represented by the mentioned kernel, with arbitrary size, was used. The kernel values are obtained according to Pascal's triangle. In this research, the size of its kernel is arbitrarily set to (3x3x3). The use of others size Gaussian kernel it is not recommended because it can modify the optimal structure of this kind of filter.
- Seed localization. This is a critical step due the multiple presences of LES. For seed coordinates calculation we develop a general pipeline using the next techniques:
 - RGB to gray transformation. Take into account the biological approach proposed in [10], the original RGB images were transformed to gray images. For this, the Equation (1) was used.

$$I_{\text{gray}} = 0.2989\mathbf{R} + 0.5870\mathbf{G} + 0.1140\mathbf{B} \quad (1)$$

- Canny filter. The I_{gray} is processed using Canny filter for obtaining the I_{canny} . This image is a contour map associated with the objects present in the image. First this filter smooths the I_{gray} using a discrete Gaussian filter, with standard deviation given by the I_{gray} standard deviation Then it detects local maxima and marks the position of those local maxima. The tuning parameters of this filter are the low and high thresholds [11].
- Labeling process. This process lets to obtain a labeled image (I_{lab}). Each one of the edges in I_{canny} is labeled in order to reduce the structures that no belong to LES.
- Generalized Hough transformation (GHT). The GHT is a smart operator and it is described in [12]. For seed localization we develop a technique, based on GHT, structured in two stages: training and detection. For the training image, a map of labeled contours and prototypes of the LES was obtained. For each point of the prototypes, determine the parameters: radial distance (r) to the centroid, angular orientation (α) with respect to the horizontal and the angle (θ) formed by the tangents at each point of each prototype and the horizontal Cartesian axis. Using θ , r and α

look up table (LuT) was constructed. For each detection image, a binary contour map was generated, estimating the angle θ_v at each point. The centers that the candidates can be calculated by looking in the LuT the r and α that met the condition $\theta_v = \theta$. The location of each candidate was increased in the parameters arrangement, determining the center and the most voted "label". Thus, extracting the seeds for the subsequent segmentation of the LES.

2.2.2. Segmentation. This stage involves two steps: seed point detection and RG segmentation technique. These steps are presented at next.

- Region growing technique (RG). The RG technique applied in this work uses the confidence connected approach for LES segmentation. For RG, the seeds voxels necessities for RG initialization are provided by the GHT. They are used as the initial position for start growing the initial neighborhood, which has an arbitrary size (s). The criterion for including new voxels in the region is defined by an intensity range around the mean value of the voxels existing in this region. The extent of the densitometric information interval is computed as the product of the variance image and an arbitrary multiplier (m) [13].

During the tuning process, the LES segmented are compared with the ground truths traced by clinic specialist. The Dice score (Ds) is used in order to estimate the difference between these structures [14]. The Ds is a metric with values between zero and 1. This metric is better when its value is closest to 1. Additionally, the areas and perimeters of segmented structures are calculating in order to build a LES characterization.

3. Results

A maximum Ds of 0.85 is obtained from the tuning, which generated the optimal parameters for RG technique ($m = 7.0$ and $s = 1$). Figure 3 shows an axial view of an original image and the images linked to digital processing developed with the SACS.

Finally, Table 1 shows the perimeter and area values considering LES semi-automatic segmentation.

Table 1. Clinical parameters associated with segmented LES.

LES Label Images	Area (μm^2)-Perimeter(μm)
D1_1	41.22-25.24
D1_2	22.26-19.39
D1_3	46.20-27.33
D2_1	46.86-26.29
D2_2	55.93-34.23
D3_1	60.58-31.63
D4_1	42.37-25.62
D5_1	61.77-30.18
D6_1	61.30-29.51

The values reported in Table 1 are similar that the values reported in reference [2]. Additionally, in a medical image segmentation context, the Ds is used for comparing manual and automatic segmentation. The interpretation of Ds values is: the manual segmentation and the automatic one matching when the Ds is 1 and they no matching at all when the Ds is zero. In this sense, normally, values of Ds over 0.75 are good accepted, in the medical routine. In this sense, according to the results of this research, the SACS had a good performance segmenting lungs because the maximum Ds value obtained for the lung segmentation was 0.85.

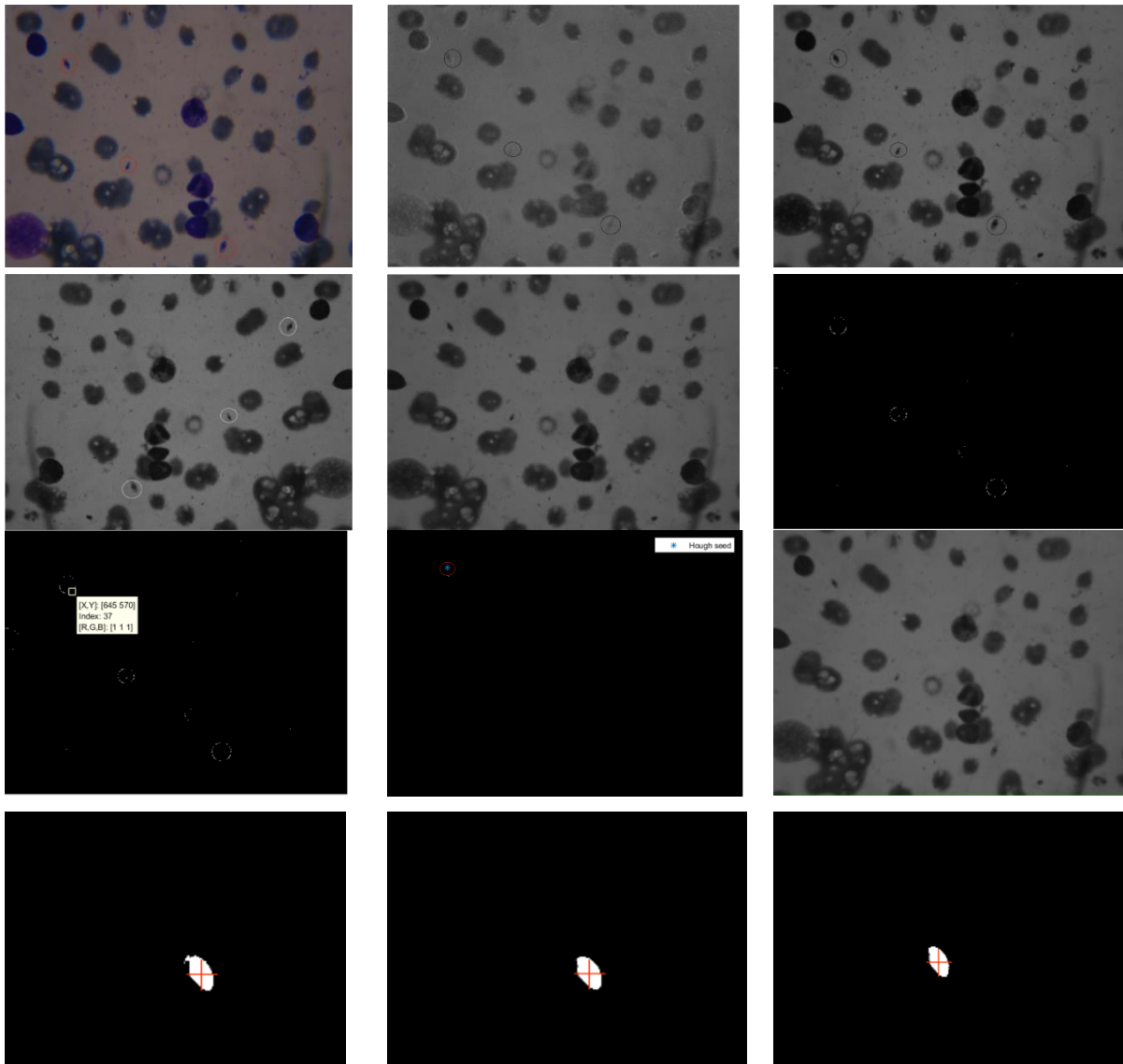


Figure 3. Axials views about effect of the SACS over microscopic leishmaniasis images. The description will be done considering left to right figure orientation and take into account each image in the rows of this figure. Top row: Original RGB, Blue channel and Green channel. Second row: Red channel, Gray intensity and Canny. Third row: Labeled, GHT and 3D Gaussian. Bottom row: The segmentation of the three parasites, present in the original image.

4. Conclusions

A semiautomatic computational technique has been presented for the LES segmentation considering color microscopic images. The generalized Hough transformation allowed the calculation of the seeds necessary for the precise segmentation of the LES. The values obtained for the D_s indicate the good performance of the proposed technique. It is planned, for the future, to use the SACS in the segmentation of an important number of datasets.

References

- [1] Longo D, Fauci A, Kasper D, Hauser S, Jameson J and Loscalzo J 2018 *Harrison's principles of internal medicine* (USA: McGraw-Hill)
- [2] Farahi M, Rabbani H, Talebi A, Sarrafzadeh O and Ensafi S 2015 Automatic segmentation of leishmania parasite in microscopic images using a modified cv level set method *Proc. SPIE* **9817** 98170K

- [3] Vera M, Huérfano Y, Gelvez E, Valbuena O, Salazar J, Molina V, Vera M I, Salazar W and Sáenz F 2019 Segmentation of brain tumors using a semi-automatic computational strategy *J. Phys.: Conf. Ser.* **1160** 012002
- [4] Tan H, Jiang H, Dong A, Yang B and Zhang L 2014 Cv level set based cell image segmentation using color filter and morphology *Proc. Int. Conf. on Information Sci. Electronics and Electrical Eng.* **3(1)** 1073
- [5] Yang L, Meer P and Foran D 2005 Unsupervised segmentation based on robust estimation and color active contour models *IEEE Trans. on Inf. Tech. in Biomedicine* **9(3)** 475
- [6] Sadeghian F, Seman Z, Ramli A, Kahar B and Saripan M 2009 A framework for wbc segmentation in microscopic images using digital image processing *Biological procedures online* **11** 196
- [7] Górriz M, Aparicio A, Raventós B, Vilaplana V, Sayrol E and Lopez D 2018 Leishmaniasis parasite segmentation and classification using deep learning *Proc. 10th International Conference: AMDO (Berlín Springer)* **43956** 53
- [8] Farahi M, Rabbani H and Talebi A 2014 Automatic boundary extraction of leishman bodies in bone marrow samples from patients with visceral leishmaniasis. *J. Isfahan. Med. Sch.* **32(286)** 726
- [9] Koenderink J 1984 The structure of images *Biol. Cybern.* **50** 363
- [10] Zhigan N, Wenbin S and Xiong C 2015 Adhesion ore image separation method based on concave points matching *Proc. International Conference on Information Technology and Intelligent Transportation Systems 2* (China: Springer)
- [11] Ibañez L 2004 *The ITK software guide* (USA: Kitware Inc.)
- [12] Vera M, Bravo A and Medina R 2011 Improving ventricle detection in 3d cardiac multislice computerized tomography images *Proc. Computer Vision, Imaging and Computer Graphics. Theory and Applications. Communications in Computer and Information Science* ed Richard P and Braz J **229**. (Berlin: Springer Heidelberg)
- [13] Vera M, Medina R, Del Mar A, Arellano J, Huérfano Y and Bravo A 2019 An automatic technique for left ventricle segmentation from msct cardiac volumes *J. Phys.: Conf. Ser.* **1160** 012001
- [14] Dice L 1945 Measures of the amount of ecologic association between species *Ecology* **26(3)** 29